Supplementary Information for manuscript

Spint1 disruption in mouse pancreas leads to glucose intolerance and impaired insulin production involving HEPSIN/MAFA.

Hsin-Hsien Lin, et al.

Table of content

Supplementary Figures

Supplementary Figure 1

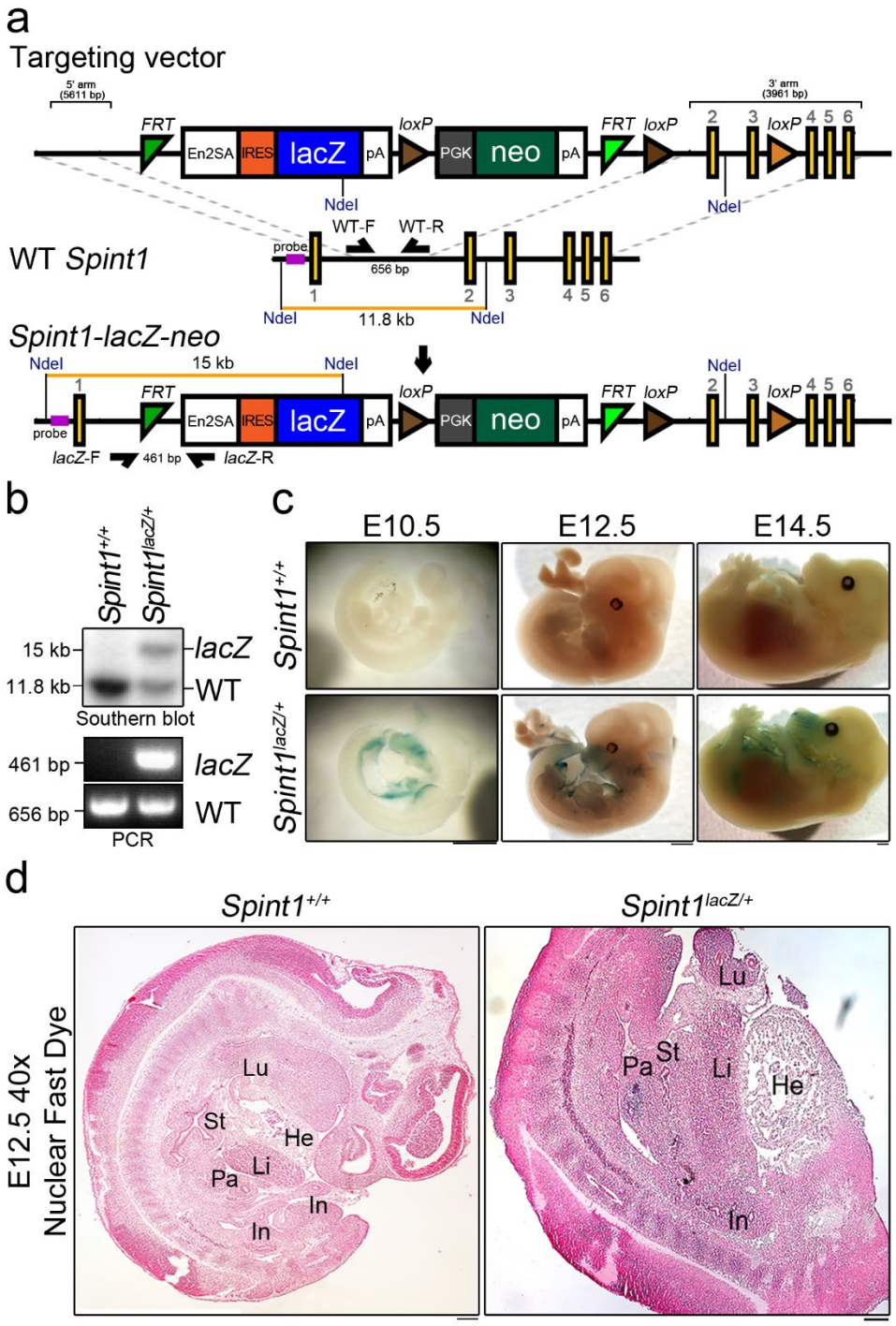

Supplementary Fig. 1. Spatiotemporal expression patterns of *Spint1-lacZ* during *Spint1*$^{lacZ/+}$ mouse embryo development.

a, Generation of *Spint1*$^{lacZ/+}$ mice. Maps of the targeting vector (upper), wild-type *Spint1* allele (WT *Spint1*, middle), and recombinant allele in the *Spint1* intron 1 (*Spint1-lacZ-neo*, lower). The *lacZ-neo* fusion cassette was inserted into the first intron of *Spint1 via* homologous recombination. An extra NdeI site in *lacZ* cDNA enabled the distinction between wild-type and recombinant alleles using Southern blotting. Probe: a 5' probe used for Southern blotting. WT-F and WT-R: the primer pair for wild-type *Spint1* allele. *lacZ*-F and *lacZ*-R: the primer pair for *Spint1-lacZ* allele. 1-6: the exons of *Spint1*. *FRT* and *loxP*: flippase and Cre recognition sites, respectively. **b,** Southern blotting and genotyping for wild-type and *Spint1*$^{lacZ/+}$ embryonic stem (ES) cells and mice. Wild-type *Spint1* (*Spint1*$^{+/+}$) and recombinant *Spint1*$^{lacZ/+}$ ES cell clones were determined using Southern blotting. The probe is described in Supplementary Fig. 1**a**. The sizes of NdeI-cleaved fragments of *Spint1*$^{+/+}$ and *Spint1*$^{lacZ/+}$ alleles were approximately 11.8 kb and 15 kb, respectively (upper panel). Moreover, PCR-based genotyping was performed using mouse tail DNAs and the wild-type (WT) and *lacZ* primer pairs described in Supplementary Fig. 1**a**. The PCR products for wild-type and *Spint1-lacZ* alleles were 656 bp and 461 bp in size after agarose electrophoresis, respectively. **c,** Representatives of E10.5, E12.5, and

E14.5 whole-mount LacZ-stain embryos from wild-type (*Spint1*$^{+/+}$) and *Spint1*$^{lacZ/+}$ mice. Scale bar, 200 μm. (n= 4 per group). **d,** Representative histology images of LacZ-stained E12.5 *Spint1*$^{lacZ/+}$ and *Spint1*$^{+/+}$ embryos. The LacZ-stained E12.5 *Spint1*$^{lacZ/+}$ and *Spint1*$^{+/+}$ mouse embryos were sectioned *sagittally* and counterstained with nuclear fast red. Lu: Lung, St: Stomach, He: Heart, Li: Liver, Pa: Pancreas, In: Intestine. Scale bar, 100 μm. Source data are provided as a Source Data file.

Supplementary Figure 2

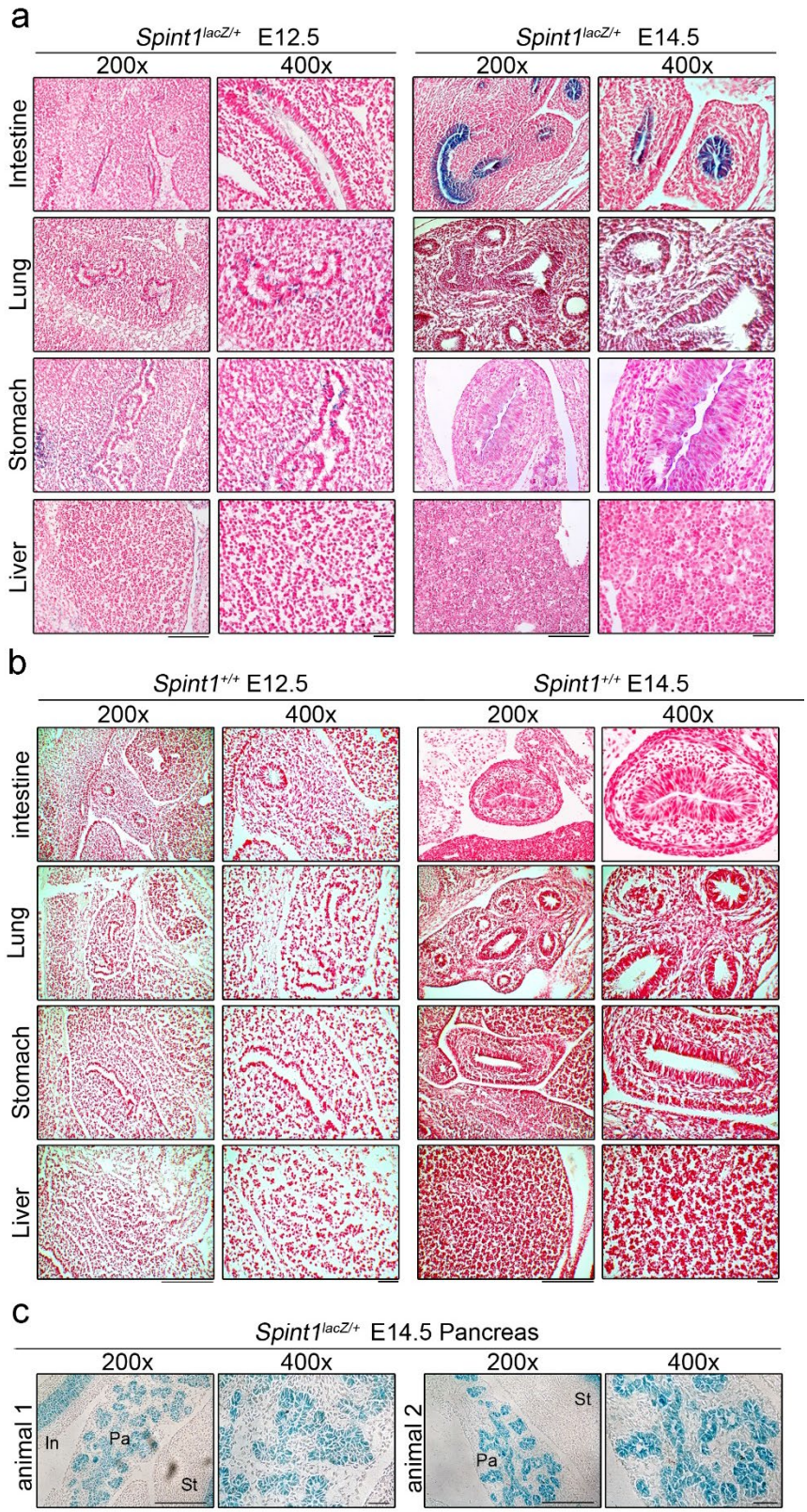

Supplementary Fig. 2. The *Spint1-lacZ* expression patterns in the embryonic

intestine, lung, stomach, liver, and pancreas in *Spint1*$^{+/+}$ and *Spint1*$^{lacZ/+}$ mouse embryos.

a, Expression levels of *Spint1-lacZ* in the intestine, lung, stomach and liver in E12.5 and E14.5 *Spint1*$^{lacZ/+}$ embryos after X-gal staining. Mouse E12.5 and E14.5 *Spint1*$^{lacZ/+}$ embryos were incubated with an X-gal solution to reveal LacZ activity. After incubation, embryos were dissected and counterstained by nuclear fast red. **b,** Images of the intestine, lung, stomach, and liver in E12.5 and E14.5 *Spint1*$^{+/+}$ embryos after X-gal-staining. Representative X-gal-stained embryo sections were counterstained by nuclear fast red. These images were used as controls for Supplementary Fig. 2**a**. **c,** High expression levels of *Spint1-lacZ* in the E14.5 pancreas of two different embryos. Representative microscopic images of pancreatic sections of X-gal-stained E14.5 *Spint1*$^{lacZ/+}$ embryos without counterstaining. In: Intestine, St: Stomach, Pa: Pancreas. The results showed that the whole primordial pancreatic duct and acini-like structures exhibited strong lacZ signals. Scale bar, 100 μm for 200× panels; 20 μm for 400× panels.

Supplementary Figure 3

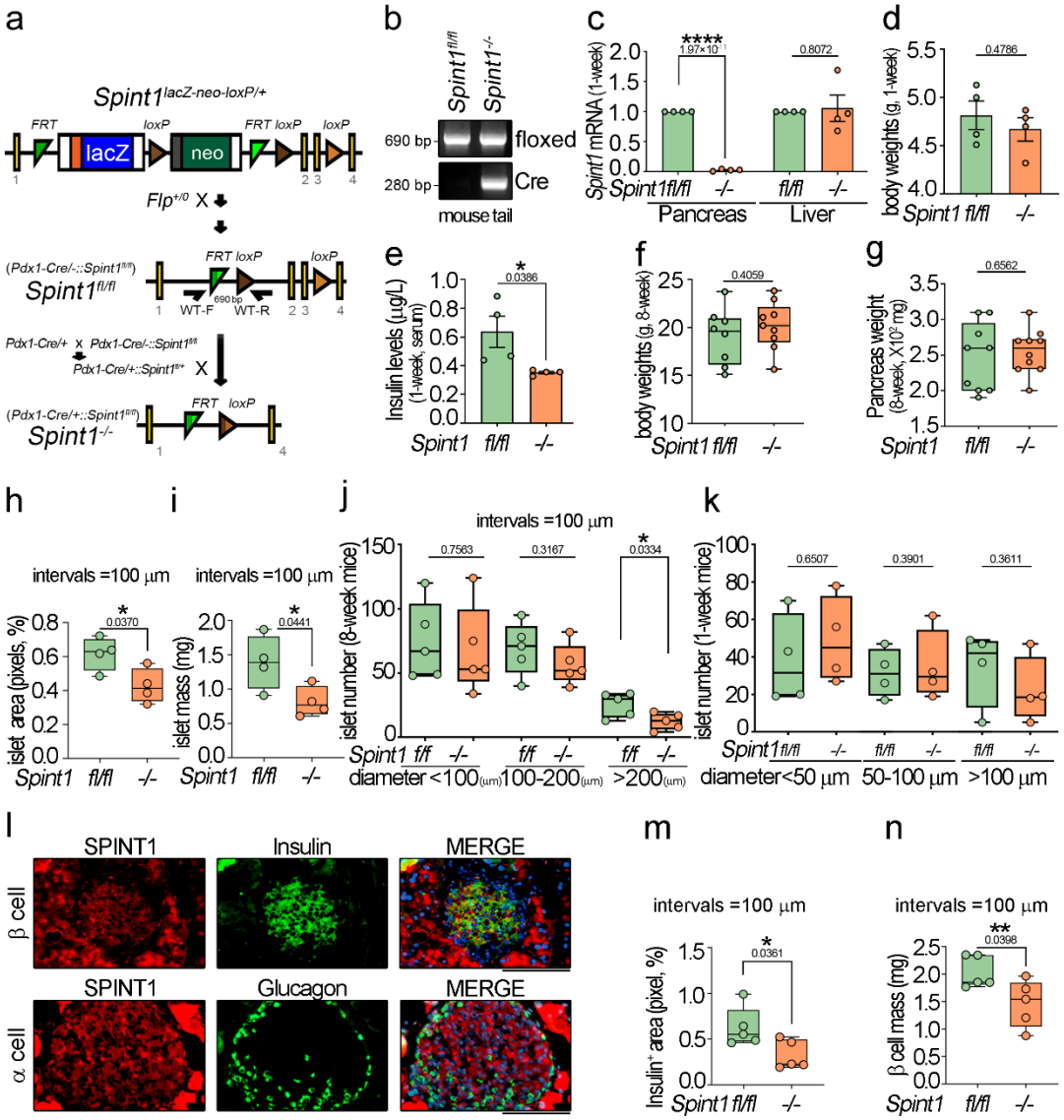

Supplementary Fig. 3. Phenotypic characteristics of 1-week-old and 8-week-old mice with pancreas-specific *Spint1* deficiency.

a, Generation of pancreas-specific *Spint1*-deficient (*Spint1*$^{-/-}$) mice. The *Spint1*$^{lacZ\text{-}neo\text{-}loxP/+}$ mice, harboring the recombinant allele *Spint1-lacZ-neo* (top), were mated with FLP-expressing mice (*Flp*/+) to remove the *lacZ* reporter cassette and generate the

loxP-floxed wild-type *Spint1* control mice (*Spint1*$^{fl/fl}$, middle). For generating the pancreas-specific *Spint1*-deficient mice (bottom), the *Spint1*$^{fl/fl}$ mice were crossed with *Pdx1-Cre/+* mice to delete exons 2 and 3 in the mouse pancreas, resulting in the generation of *Pdx1-Cre/+::Spint1*$^{fl/fl}$ (namely *Spint1*$^{-/-}$) mice. **b,** Genotyping for *Spint1*$^{fl/fl}$ and *Spint1*$^{-/-}$ mice. Primers WT-F and WT-R (depicted in Supplementary Fig. 1**a**) were used to amplify the *lacZ-neo* reporter-deleted intron 1 region in the floxed wild-type allele, employing mouse tail DNA. The sizes of the floxed wild-type *Spint1* PCR product and *Cre* PCR product were 690 bp and 280 bp, respectively. **c,** Validation of *Spint1* expression in the pancreas and livers of 1-week-old *Spint1*$^{-/-}$ mice using Q-RT-PCR. The pancreas (left) and liver (right) were isolated from 1-week-old *Spint1*$^{fl/fl}$ and *Spint1*$^{-/-}$ mice and subjected to RNA extraction and reverse transcription. The mRNA levels of *Spint1* were measured using Q-RT-PCR with normalization to *Gapdh* (4 mice per group). **d,** Body weights analysis of 1-week-old *Spint1*$^{fl/fl}$ and *Spint1*$^{-/-}$ mice (n= 4 mice per group). **e,** Examination of the serum insulin levels in 1-week-old *Spint1*$^{fl/fl}$ and *Spint1*$^{-/-}$ mice using an ELISA kit (4 mice per group). **f,** Body weights analysis of 8-week-old *Spint1*$^{fl/fl}$ and *Spint1*$^{-/-}$ mice (n= 8 for *Spint1*$^{fl/fl}$ mice and n= 9 for *Spint1*$^{-/-}$ mice). **g,** Pancreas weights analysis of 8-week-old *Spint1*$^{fl/fl}$ and *Spint1*$^{-/-}$ mice (n= 9 for *Spint1*$^{fl/fl}$ mice and n= 10 for *Spint1*$^{-/-}$ mice). **h-j,** Quantification of islet area percentage, islet mass, and islet numbers in 8-week-old

95 *Spint1*$^{-/-}$ and *Spint1*$^{fl/fl}$ mice using sections taken at 100 μm intervals throughout the
96 whole mouse pancreas. **h,** Each pancreas underwent serial sections (300 sections per
97 pancreas), and one out of every 20 serial sections (100 μm intervals for each section)
98 was taken for H&E staining to reveal islet areas. ImageJ determined the percentage of
99 islet area in a whole pancreas area based on the merged full-view microscopic images
100 of 15 sections per mouse (4 mice per group). **i,** The islet mass was calculated by
101 multiplying the islet area percentage in **h** by pancreas weight in **g** (n = 4 per group). **j,**
102 Islet number quantification in the pancreas of 8-week-old *Spint1*$^{fl/fl}$ and *Spint1*$^{-/-}$ mice.
103 The islets with a diameter below 100 μm were defined as small islets, those with a
104 diameter between 100 μm and 200 μm as medium islets, and those with a diameter
105 above 200 μm as large islets. The islet diameters were measured using ImageJ from
106 H&E-stained microscopic images, with one section selected from every 20 serial
107 sections (300 sections per pancreas), comprising 15 sections per mouse and four mice
108 per group. **k,** Islet number quantification in the pancreas of 1-week-old *Spint1*$^{fl/fl}$ and
109 *Spint1*$^{-/-}$ mice. The islets with a diameter below 50 μm were defined as small islets,
110 those with a diameter between 50 μm and 100 μm as medium islets, and those with a
111 diameter above 100 μm as large islets. The islet diameters were measured using
112 ImageJ from H&E-stained microscopic images, with one section selected from every
113 20 serial sections (300 sections per pancreas), comprising 15 sections per mouse and 4

mice per group. **l,** Immunofluorescence images of SPINT1, glucagon (α cell), and insulin (β cell) in mouse islets using immunofluorescence microscopy. Mouse pancreatic sections were immunohistochemically stained using an anti-SPINT1 antibody. Subsequently, the sections were stripped, followed by immunofluorescent staining using anti-glucagon or anti-insulin antibodies (detailed procedures in Method sections). The IHC results of SPINT1 were pseudo-colored in red (left panels), while insulin or glucagon was visualized by fluorochrome-labeled secondary antibody (green, middle panels). Nuclei were counterstained with DAPI (blue). Their merged images were shown in the right panels. Scale bar, 20 μm. **m-n,** Quantification of percentages of the insulin-positive area and β cell mass in 8-week-old *Spint1*$^{fl/fl}$ and *Spint1*$^{-/-}$ mice, using sections taken at 100 μm intervals throughout the whole mouse pancreas. **m,** Each pancreas underwent serial sections (300 sections per pancreas) in which one out of every 20 serial sections (100 μm intervals for each section) was taken for immunohistochemical stained using an anti-insulin antibody and were determined based on the merged full-view microscopic images of 15 sections per mouse (4 mice per group) using ImageJ. **n,** The β cell mass was calculated by multiplying the insulin-positive area percentage in **k** by the pancreas weight in **g**. Statistical significance was assessed using a two-tailed Student's *t*-test for all panels. For bar plots, bars are represented as mean ± SEM. In the box plots, the boxes span

from the 25th to the 75th percentiles, with a line indicating the median. Whiskers extend to values within 1.5 times the interquartile range, defined as the difference between the 25th and 75th percentiles. *, P <0.05; **, P <0.01; ****, P <0.001. Below the asterisks are the precise statistical results. Source data are provided as a Source Data file.

Supplementary Figure 4

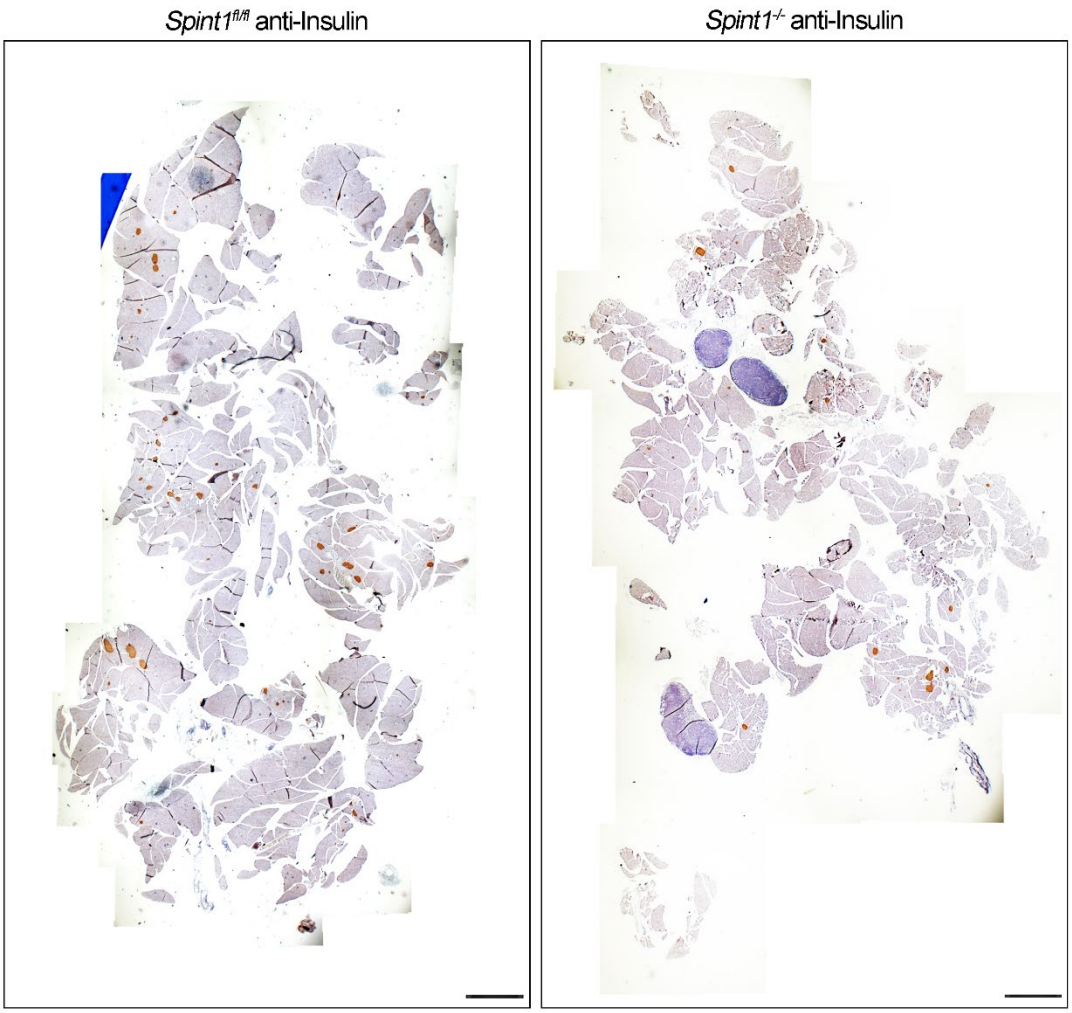

Supplementary Fig. 4. Representative full-view images of 8-week-old *Spint1*$^{fl/fl}$ and *Spint1*$^{-/-}$ pancreatic sections after immunohistochemical staining using an anti-insulin antibody.

The pancreas sections of 8-week-old *Spint1*$^{fl/fl}$ and *Spint1*$^{-/-}$ mice were immunohistochemically stained using an anti-insulin antibody and counterstained with hematoxylin. All the low-power filed images taken from the same slide of the pancreas were merged using Photoshop software to restore the complete view of the

147 pancreas. The area of whole pancreas in this study was calculated based on the full-

148 view images. Scale bar, 250 mm.

149

Supplementary Figure 5

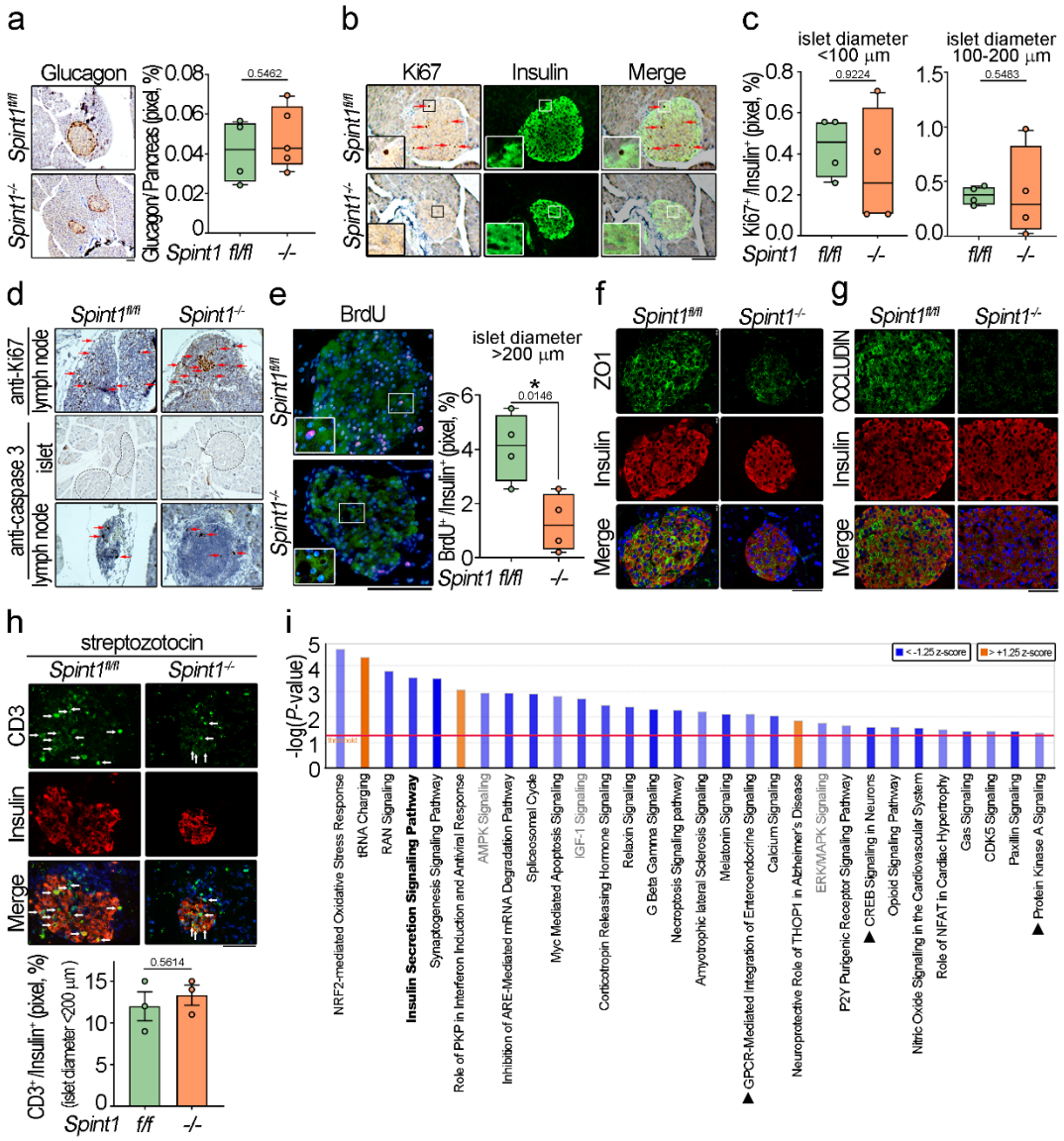

Supplementary Fig. 5. Islet phenotypes in 8-week-old mice with pancreas-specific *Spint1* deficiency analyzed through proliferation and apoptosis markers, tight junction proteins, and islet CD3$^+$ cells percentage.

a, Percentages of glucagon-positive areas in the pancreas of 8-week-old *Spint1*$^{fl/fl}$ and *Spint1*$^{-/-}$ mice. Pancreatic sections were immunohistochemically stained for glucagon (α cell) and counterstained with hematoxylin. Glucagon-positive areas in the pancreas

were analyzed using ImageJ, with percentages calculated by dividing glucagon-positive pixels by total pancreas pixels (3 sections per pancreas and four mice per group). Representative microscopic images were shown in the left panel. Scale bar, 20 μm. **b,** Detection of Ki67-positive β cells in the pancreatic islets of 8-week-old *Spint1*$^{fl/fl}$ and *Spint1*$^{-/-}$ mice. Pancreatic sections underwent IHC using an anti-Ki67 antibody (left panel) and subsequent immunofluorescence microscopy using an anti-insulin antibody (middle panel). Ki67-positive β cells are shown in the merged images (right panel). Scale bar, 20 μm. High-magnification images are shown in the insets at the lower left corner of each panel. **c,** The percentages of Ki67^{+} β cells in the small-diameter islets (< 100 μm) and medium-diameter (100-200 μm) of 8-week-old *Spint1*$^{fl/fl}$ and *Spint1*$^{-/-}$ mice. The percentages of Ki67^{+} β cells (detected by insulin expression) in the medium and small islets of the pancreas were statistically calculated from 6 sections under 300 μm intervals per pancreas (4 mice per group) and shown in the left and right panels. The percentages of large islets (islet diameter > 200 μm) are shown in Fig. 2**d**. **d,** Detection of caspase 3 and Ki67 in the lymph nodes or islets of 8-week-old *Spint1*$^{fl/fl}$ and *Spint1*$^{-/-}$ mice. Representative immunohistochemistry images of Ki67 and caspase 3 in the lymph nodes or islets of *Spint1*$^{fl/fl}$ and *Spint1*$^{-/-}$ mice are presented. As some caspase-3-positive signals in the mouse lymph nodes (bottom panel), no definite caspase 3 signal can be seen in the

177 pancreatic islets (middle panel) of *Spint1*$^{fl/fl}$ and *Spint1*$^{-/-}$ mice (3 sections per pancreas
178 and three mice per group). Scale bar, 20 μm. **e,** Analysis of bromodeoxyuridine
179 (BrdU) incorporation rate in the pancreatic β cells of 8-week-old *Spint1*$^{fl/fl}$ and *Spint1*$^{-/-}$
180 mice. Mice were daily treated with sterile drinking water containing BrdU (1
181 mg/mL) for 14 days. Representative images after immunofluorescence microscopy
182 showed the merged signals for BrdU (pink), insulin (green), and DAPI (blue) in the
183 left panel. Scale bar, 20 μm. The rates of BrdU incorporation in β cells were
184 quantified in the large pancreatic islets [6 sections per pancreas (300 μm intervals)
185 and four mice per group], as shown in the right panel. High-magnification images are
186 shown in the insets at the lower left corner of each panel. **f-g,** Immunofluorescence
187 analysis of ZO1 (**f**) and OCCLUDIN (**g**) in the pancreatic islets of 8-week-old
188 *Spint1*$^{fl/fl}$ and *Spint1*$^{-/-}$ mice. Mouse pancreatic sections were subjected to
189 immunofluorescence microscopy to detect ZO1 (green) or OCCLUDIN (green) in
190 insulin-positive (red) cells (3 sections per mouse, 3 mice per group). Nuclei were
191 counterstained with DAPI (blue). Scale bar, 20 μm. **h,** Analysis of $CD3^+$ immune cells
192 in the pancreatic islets of *Spint1*$^{fl/fl}$ and *Spint1*$^{-/-}$ mice following streptozotocin
193 treatment. After streptozotocin treatment in Fig. 2**k**, the mouse pancreatic sections
194 were subjected to immunohistochemical staining to detect $CD3^+$ immune cells (green)
195 among $insulin^+$ regions (red). White arrows mark the $Ki67^+$ β cells in the CD3 and

196 merge images. Nuclei were counterstained with DAPI (blue). Scale bar, 20 μm. The
197 percentages of $CD3^+$ cells relative to $insulin^+$ regions (3 sections per mouse, 3 mice
198 per group) are presented in the bottom panel. **i,** Ingenuity Pathway Analysis (IPA) of
199 the differential protein profiles in *Spint1*$^{-/-}$ islets compared to *Spint1*$^{fl/fl}$ islets. Thirty
200 signal pathways were identified under the criteria of the −log (*P*-value) value over
201 1.25. Statistical analysis was performed using a two-sided Fisher's exact test, and the
202 false discovery rate was controlled using the Benjamini-Hochberg procedure to
203 correct *P* values. The down-regulated pathways in *Spint1*$^{-/-}$ islets compared to
204 *Spint1*$^{fl/fl}$ islets are highlighted by blue bars, while orange ones indicate the up-
205 regulated pathways. Black triangles mark GPCR, CREB, and PKA signaling
206 pathways. Statistical significance was assessed using a two-tailed Student's *t*-test for
207 **a**, **c**, **e** and **h**. For bar plots, bars are represented as mean ± SEM. In the box plots, the
208 boxes span from the 25th to the 75th percentiles, with a line indicating the median.
209 Whiskers extend to values within 1.5 times the interquartile range, defined as the
210 difference between the 25th and 75th percentiles. *, $P < 0.05$. Below the asterisks are
211 the precise statistical results. Source data are provided as a Source Data file.

Supplementary Figure 6

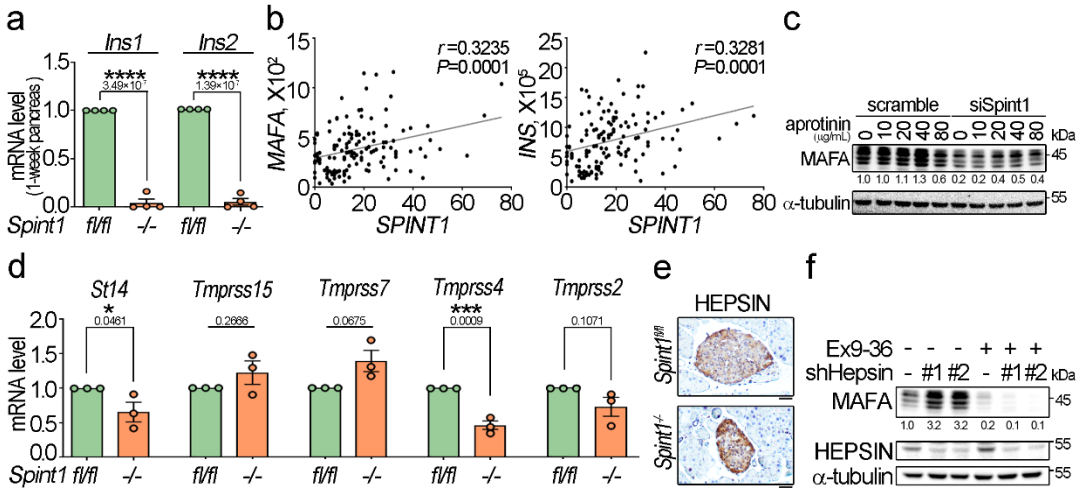

Supplementary Fig. 6. Analysis of the expression levels of *Ins1*, *Ins2*, selected serine proteases, and HEPSIN in *Spint1*$^{fl/fl}$ and *Spint1*$^{-/-}$ mouse pancreas/islets, the effect of aprotinin, *Hepsin* silencing, and Ex9-36 on the MAFA protein levels, as well as correlations between *SPINT1* and *MAFA*/*INS* expression in human β cells.

a, Analysis of *Ins1* and *Ins2* expression levels in the pancreas of 1-week-old *Spint1*$^{fl/fl}$ and *Spint1*$^{-/-}$ mice. Mouse pancreas RNAs were extracted and subjected to Q-RT-PCR analysis with normalization to *Gapdh* (n= 4 mice per group). The results showed that the expression levels of *Ins1* and *Ins2* were significantly reduced in the pancreas of 1-week-old *Spint1*$^{-/-}$ mice compared to *Spint1*$^{fl/fl}$ mice. **b,** Correlation of the expression levels between *SPINT1* and *MAFA* (left panel) and between *INS* and *SPINT1* (right panel) in human pancreatic islets using the GSE164416 dataset. The Pearson

correlation coefficients (*r*) are shown in figures (n= 133 per group) and statistical significance was determined using a two-sided Pearson's correlation test. Gray lines represent the linear regression line. **c,** Effect of a broad serine protease inhibitor, aprotinin, on the expression of MAFA in *Spint1*-silenced NIT-1 cells. NIT-1 cells were transfected with siSpint1 or scramble siRNA and then incubated with regular culture media in the presence of 0, 10, 20, 40, and 80 μg/mL aprotinin for 24 hours. Cell lysates were collected and subjected to immunoblot analysis using an anti-MAFA antibody. α-tubulin was used as a loading control. The intensities of MAFA bands were measured using ImageJ, normalized to α-tubulin, and statistically calculated from three independent experiments. The mean values relative to the control of scramble siRNA without aprotinin are presented at the bottom of the MAFA image. **d,** Q-RT-PCR analysis of *St14* (matriptase), *Tmprss15*, *Tmprss7*, *Tmprss4*, and *Tmprss2* mRNA levels in 8-week-old *Spint1*$^{fl/fl}$ and *Spint1*$^{-/-}$ mouse islets. Isolated mouse islets were subjected to RNA extraction and Q-RT-PCR with normalization to *Gapdh.* The expression levels of each gene were statistically calculated from three independent experiments (n= 3 mice per group). **e,** IHC analysis of HEPSIN in the pancreas of *Spint1*$^{fl/fl}$ and *Spint1*$^{-/-}$ mouse islets. Mouse pancreas samples were immunohistochemically stained, and representative images are shown here. The results were further statistically calculated for HEPSIN expression and shown in Fig.

4**i**. Scale bar, 20 μm. **f,** Ex9-36 treatment reversed the effect of *Hepsin* silencing on MAFA expression. NIT-1 cells were infected with two different *Hepsin*-targeting shRNAs (shHepsin #1 and #2) lentivirus for 48 hours and then treated with GLP1R antagonist Ex9-36 for 24 hours. Cell lysates were collected and subjected to western blot analysis using anti-MAFA and anti-HEPSIN antibodies, with α-tubulin serving as a loading control. Statistical significance was determined using a two-tailed Student's *t*-test for **a** and **d.** All data were represented as mean ± SEM. *, P <0.05; ***, P < 0.001; ****, P < 0.0001. Below the asterisks are the precise statistical results. Source data are provided as a Source Data file.

Supplementary Figure 7

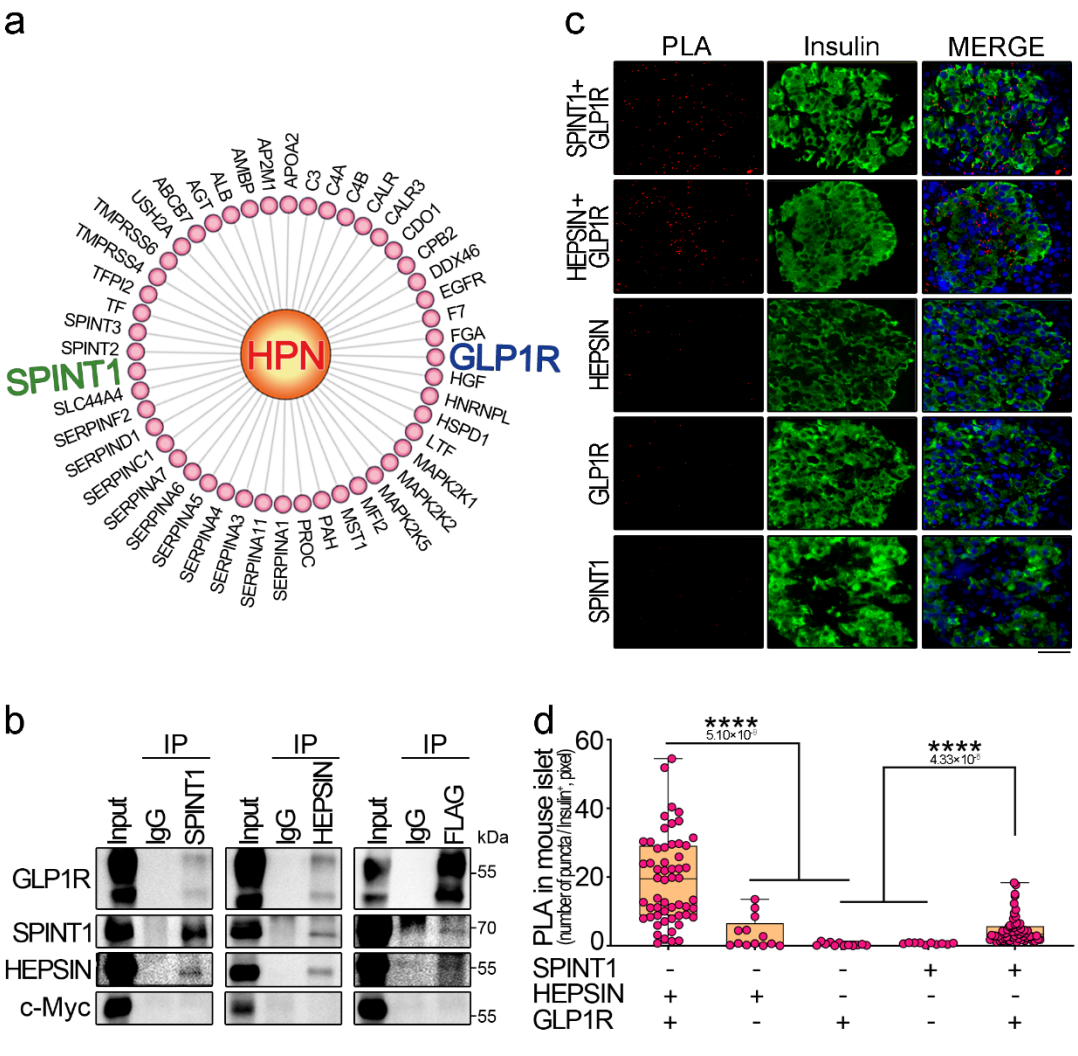

Supplementary Fig. 7. The Interactions of SPINT1, HESPIN, and GLP1R in human islets and β cells.

a, Analysis of HEPSIN interactomes using STRING database (http://string-db.org). The results revealed many potential HEPSIN-interacting proteins; among them, GLP1R caught our attention because of its important role in pancreatic β cells. **b,** Determination of SPINT1, HEPSIN, and GLP1R interactions in a complex using co-

immunoprecipitation assays. HEK293T cells were transiently transfected with *Spint1*, *Hepsin*, and *Glp1r* plasmids. Cell lysates were then subjected to immunoprecipitation (IP) using anti-SPINT1 (left panel), anti-HEPSIN (middle panel), and anti-FLAG-tag antibodies (right panel, for N-terminally FLAG-tagged GLP1R). IgG served as IP control. Immunoprecipitated proteins were then subjected to immunoblotting using anti-SPINT1, anti-HEPSIN, and anti-FLAG-tag antibodies, with c-Myc as input control. **c,** Examination of the protein-protein interaction among SPINT1, HEPSIN, and GLP1R in human islets using the proximity ligation assay (PLA). Human pancreatic sections were subjected to PLA using two pairs of primary antibodies: anti-GLP1R *vs.* anti-SPINT1 and anti-GLP1R *vs.* anti-HEPSIN. Positive interaction signals in PLA were visualized as red puncta. The samples were also immunohistochemically stained using an anti-insulin antibody (green). Nuclei were counterstained with DAPI (blue). A set of representative images after the PLA analysis was shown. Scale bar, 20 μm. **d,** Quantification of PLA results in human islets in **c**. The red puncta in insulin-positive areas were counted and statistically calculated from three independent experiments using a two-tailed Student's *t*-test. In the box plots, the boxes span from the 25th to the 75th percentiles, with a line indicating the median. Whiskers extend to values within 1.5 times the interquartile range, defined as the difference between the 25th and 75th percentiles. ****, $P <$

285 0.0001. Below the asterisks are the precise statistical results. Source data are provided

286 as a Source Data file.

Supplementary Figure 8

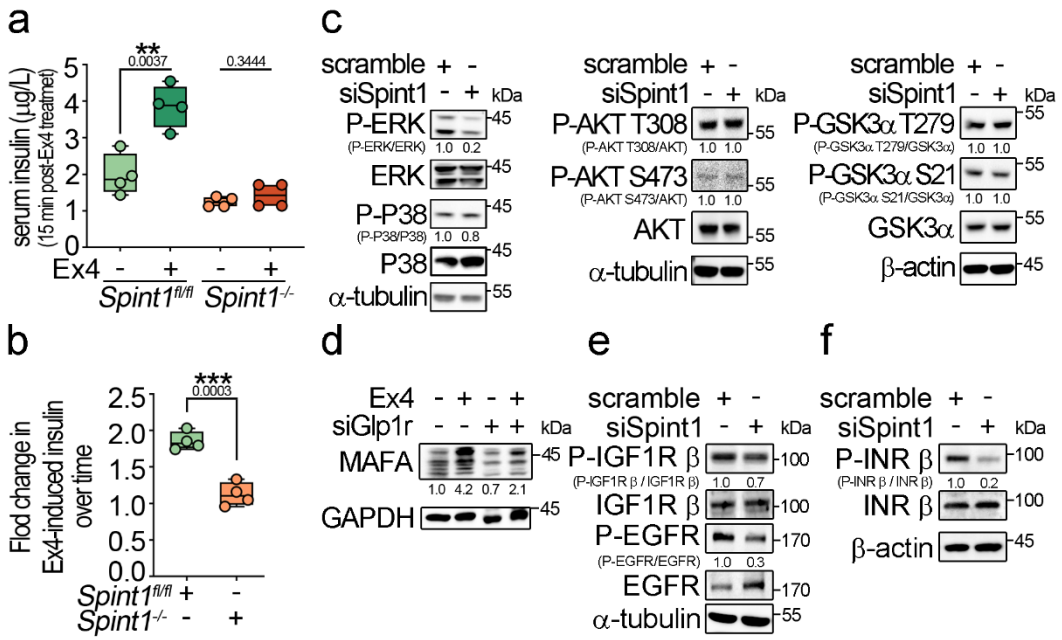

Supplementary Fig. 8. Examination of the Extendin-4 inducing insulin levels in *Spint1* knockout mice and exploring the roles of SPINT1 and HEPSIN in GLP1R-related signaling pathways.

a, Effect of Ex4 on upregulating insulin level in *Spint1*$^{fl/fl}$ and *Spint1*$^{-/-}$ mice 15 minutes post-administration. We injected Ex4 into mice following oral gavage of glucose. Details of the experimental procedure are provided in Fig. 6**k**. Insulin levels were measured 15 minutes post-administration using an ELISA kit (n = 4 per group). **b,** Ex4-induced fold change in time-integrated insulin increases in *Spint1*$^{fl/fl}$ and *Spint1*$^{-/-}$ mice described in Fig. 6**l**. Ex4 upregulated the normalized insulin response over time (represented by insulin AUC/ β cell mass) approximately twofold in *Spint1*$^{fl/fl}$ mice compared to that in *Spint1*$^{-/-}$ mice after Ex4 treatment. **c,** *Spint1*

301 silencing on the phosphorylation levels of ERK, P38, AKT, and GSK3α in NIT-1
302 cells. Cells were transfected with siSpint1. Scramble RNAs were used as a control.
303 Two days after transfection, cell lysates were collected and subjected to western blot
304 analysis using anti-phospho-ERK, anti-ERK, anti-phospho-P38, anti-P38, anti-
305 phospho-AKT(T308), anti-phospho-AKT(S473), anti-AKT, anti-phosphoGSK3α
306 (T279), anti-phospho-GSK3α (S21) and anti-GSK3α antibodies. α-tubulin and β-actin
307 served as loading controls. Western blot results were statistically calculated from
308 three independent experiments. The mean values after quantification are shown at the
309 bottom of each blot. **d,** Examination of GLP1R's role in the MAFA expression in
310 NIT-1 cells. Cells were transfected with siGlp1r or scramble RNA (control). Two
311 days after transfection, cells were treated with or without 25 nM Exendin-4 (Ex4) for
312 24 hours. Cell lysates were then collected and subjected to immunoblotting using anti-
313 MAFA and anti-GAPDH antibodies. The mean values of MAFA protein levels were
314 statistically calculated with normalization to GADPH from three independent
315 experiments using ImageJ and shown at the bottom of the MAFA blot. **e-f,**
316 Immunoblot analysis of the tyrosine phosphorylation levels of EGFR, IGF1R, and
317 INR in *Spint1*-silenced NIT-1 cells. Cells were transfected with siSpint1. Scramble
318 RNAs were used as a control. Two days after transfection, cell lysates were collected
319 and subjected to western blot analysis using anti-phosphoEGFR (P-EGFR), anti-

EGFR, anti-phosphoIGF1R (P-IGF1R), anti-IGF1R, anti-phospho-Insulin receptor (P-INR), and anti-Insulin receptor (INR). α-tubulin served as a loading control. ImageJ measured the mean values of tyrosine phosphorylation levels of these proteins with normalization to their corresponding protein levels from three independent experiments. Statistical significance was determined using a two-tailed Student's *t*-test for all panels. In the box plots, the boxes span from the 25th to the 75th percentiles, with a line indicating the median. Whiskers extend to values within 1.5 times the interquartile range, defined as the difference between the 25th and 75th percentiles. **, $P < 0.01$; ***, $P < 0.001$. Below the asterisks are the precise statistical results. Source data are provided as a Source Data file.

Supplementary Figure 9

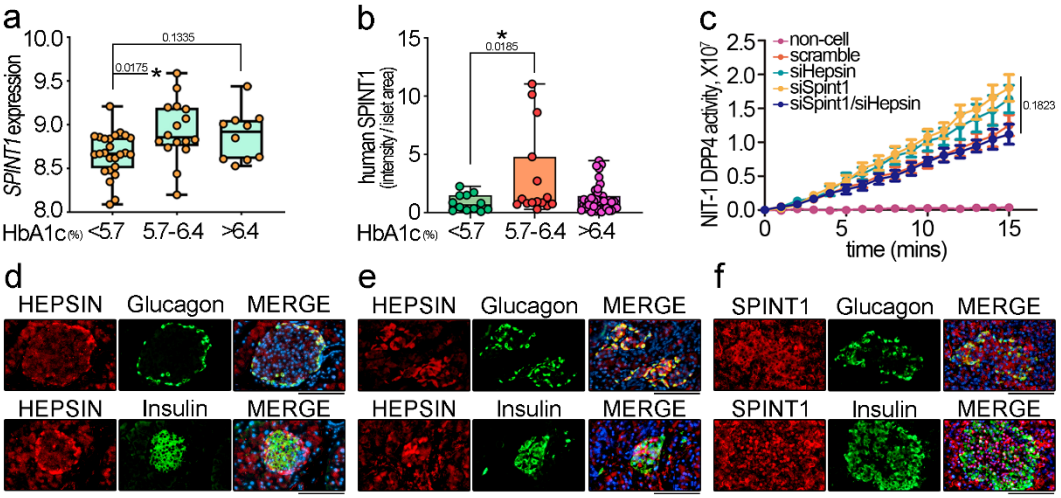

Supplementary Fig. 9. Analysis of *SPINT1* expression in human diabetes patients, DPP4 activities in *Spint1*- or *Hepsin*-silenced NIT-1 cells, and the expression patterns of SPINT1 and HEPSIN in mouse and human islets.

a, Analysis of *SPINT1* mRNA levels in prediabetes and diabetes patients. Using the GSE38642 dataset, we categorized the patients into three groups based on their blood glycated hemoglobin (HbA1c) values (orange spots) levels. Non-diabetes (n = 25): HbA1c < 5.7%, Prediabetes (n = 16): HbA1c 5.7% to 6.4%, and Diabetes (n = 10): HbA1c > 6.4%. The *SPINT1* expression levels in the human pancreas among these three groups were statistically calculated. **b,** Analysis of SPINT1 expression levels in the islets of human pancreas samples with different HbA1c levels after IHC analysis. Human pancreas samples (n=66) were obtained from the Department of Pathology, National Taiwan University Hospital. All cases were categorized into two groups

345 [undiagnosed diabetes (n = 27) and diagnosed diabetes (n = 39, HbA1c > 6.4%)]
346 according to their clinical records. The undiagnosed diabetes group was further
347 classified into two sub-groups according to their HbA1c values: HbA1c < 5.7% (n =
348 12) and HbA1c 5.7% to 6.4% (n = 15). Human pancreatic sections underwent IHC for
349 SPINT1 detection, and ImageJ was employed to measure the intensity of SPINT1
350 signals per islet. **c,** Analysis of DPP4 activities in *Spint1*- or *Hepsin*-silenced NIT-1
351 cells. NIT-1 cells were transfected with siSpint1 or siHepsin. Control cells were
352 transfected with scramble RNAs. DPP4 activities were measured every 1 minute
353 using a spectrophotometer at the wavelength 450 nm and statistically calculated from
354 three independent experiments (n = 3). **d-f,** Localization of SPINT1 and HEPSIN in
355 the α cells (glucagon) and β cells (insulin) of pancreatic islets. Mouse (**d**) and human
356 (**e** and **f**) pancreatic sections were subjected to immunofluorescence microscopy using
357 anti-SPINT1 or anti-HEPSIN antibodies, visualized as red. Nuclei were
358 counterstained with DAPI (blue). Subsequently, the samples were stripped (see
359 Methods section) and subjected to immunofluorescence microscopy for insulin
360 (green) and glucagon (green) detection. Scale bar, 20 μm. Statistical significance was
361 assessed by a one-way ANOVA with the Tukey's post-hoc test for all panels. In the
362 box plots, the boxes span from the 25th to the 75th percentiles, with a line indicating
363 the median. Whiskers extend to values within 1.5 times the interquartile range,

364 defined as the difference between the 25th and 75th percentiles. *, P <0.05. Below the

365 asterisks are the precise statistical results. Source data are provided as a Source Data

366 file.

367

Supplementary Figure 10

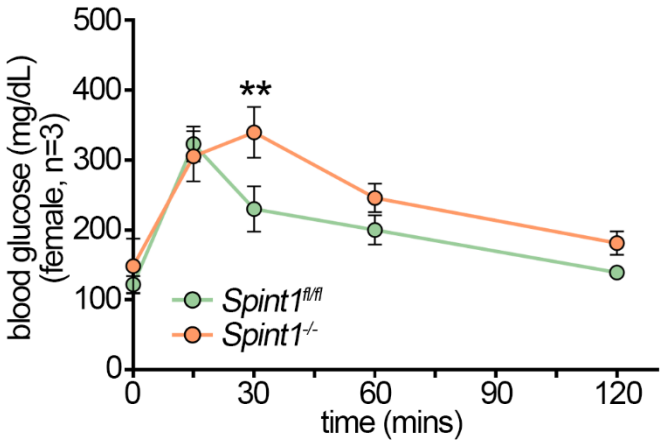

Supplementary Fig. 10. Analysis of glucose tolerance in female 8-week-old *Spint1*$^{fl/fl}$ and *Spint1*$^{-/-}$ mice.

Female mice were fasted for 8 hours and then intraperitoneally injected with 20% glucose solution (2 g/kg body weight). The tail blood samples were then taken at 15, 30, 60, and 120 minutes after injection and used to examine the glucose levels using a glucometer (n = 3 per group). A two-way ANOVA followed by Sidak's multiple comparison analysis assessed statistical significance. All data were represented as mean ± SEM. **, P <0.01. Source data are provided as a Source Data file.

Supplementary Figure 11

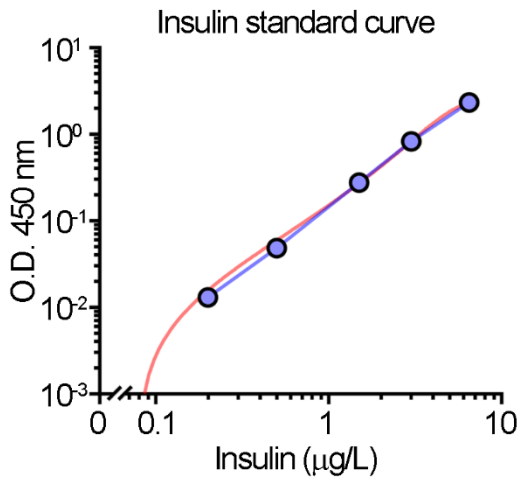

Supplementary Fig. 11. Insulin standard curve.

The logit-log plot represents the insulin ELISA standard curve, measured in quadruplicate using four-parameter logistic regression. It was generated by plotting insulin concentrations ranging from 0 to 6.5 µg/L, including values of 0.2, 0.5, 1.5, and 3.0 µg/L (n=3). Source data are provided as a Source Data file.

Supplementary Methods

Liquid chromatography with tandem mass spectrometry (LC-MS/MS)

LC-MS/MS analysis was performed on a nanoACQUITY UPLC system (Waters, Milford, MA) connected to the LTQ Orbitrap Velos hybrid mass spectrometer (Thermo Electron, Bremen, Germany) equipped with a PicoView nanospray interface (New Objective, Woburn, MA). Peptide mixtures were loaded onto a 75 μm ID, 25 cm length C18 BEH column (Waters, Milford, MA) and were separated using a segmented gradient at a 300 nl/min flow rate. Briefly, survey full scan MS spectra were acquired in the orbitrap (m/z 350–1600) with the resolution set to 60 K at m/z 400 and automatic gain control (AGC) target at 10^6. The 20 most intense ions were sequentially isolated for collision-induced dissociation MS/MS fragmentation and detection in the linear ion trap (AGC target at 10^4). Charge state screening was enabled for +2, +3, +4, and higher.

Data analysis, Functional annotation, and Ingenuity Pathway Analysis

Raw MS data were analyzed using the MaxQuant program (version 2.2.0.0). The proteins and peptides required a false discovery rate (FDR) of 0.01 and a minimum peptide length of 6 amino acids. MS/MS spectra were searched against the UNIPROTKB/SWISS-PROT database. SILAC states of peptides were determined using the MaxQuant program based on mass differences between SILAC peptide

405 pairs. Next, the information was used for searches with fixed Arg10 or Lys8
406 modifications. We chose those identified proteins present in *Spint1*$^{-/-}$/NIT-1 and
407 *Spint1*$^{fl/fl}$/NIT-1 samples for further analysis. Differentially regulated proteins were
408 sorted into two groups according to the *Spint1*$^{-/-}$/NIT-1 to *Spint1*$^{fl/fl}$/NIT-1 protein ratio
409 ($\log_2$ (ratio) > 0.5, up-regulated group; $\log_2$ (ratio) < −0.5, down-regulated). Each
410 protein group was uploaded to the Database for Annotation, Visualization, and
411 Integrated Discovery (DAVID) (https://david.ncifcrf.gov/tools.jsp) gene
412 bioinformatics resources to identify Gene Ontology (GO) terms. All annotated
413 proteins with their protein ratios were analyzed using the Ingenuity Pathway Analysis
414 (IPA) software (QIAGEN Inc., Hilden, Germany) to identify the highly regulated
415 pathways, which were ranked according to their log ratios (−log *P* value).

416 **Measurement of DPP4 activity**

417 The siRNA-transfected NIT-1 cells were replaced with serum-free media
418 containing 10 μM of a DPP4 artificial substrate (H-Gly-Pro-AMC, Merck Millipore).
419 After the administration of the DPP4 synthetic substrate, the fluorescence intensity
420 (excision wave: 360 nm; emission wave: 460 nm) was measured every minute within
421 the 15-minute period using a spectrophotometer.

422 **Co-immunoprecipitation analysis**

HEK293T cells were seeded at a density of $2x10^6$ cells in a 10-cm plate with DMEM. The next day, cells were transfected with three plasmids, each encoding *3xFlag-Glp1r-myc*, *Spint1-his-myc*, and *Hepsin-his-myc* cDNA, using Lipofectamine 3000. After 48 hours, cells were lysed using immunoprecipitation (IP) buffer (1% Triton X-100 in PBS), and cell lysates were centrifuged at 12,000 rpm at 4°C for 15 minutes. The supernatants were then collected and subjected to IP using anti-SPINT1, anti-HEPSIN, and anti-FLAG (for Flag-GLP1R protein, F3165, Sigma-Aldrich) antibodies at 4°C overnight. The samples were then incubated with protein A magnetic beads (28978116, Cytiva, USA) at 4°C for 2 hours, and the beads were then isolated using a magnetic rack. The beads were washed three times using IP buffer, and the proteins were eluted using elution buffer (1M glycine, pH 2.0). The samples were then subjected to immunoblotting analysis.

BrdU incorporation assay

Spint1$^{fl/fl}$ and *Spint1*$^{-/-}$ mice were treated with 1 mg/mL BrdU (HY-15910, MedChemExpress) in their sterile drinking water for 14 days. BrdU-containing drinking water was refreshed daily. After the BrdU treatment, mouse pancreases were isolated and subjected to immunofluorescence microscopy. Before inoculation with the anti-BrdU antibody (66241-1-lg, Proteintech), samples were incubated in 1M HCL for 30 minutes. After overnight incubation with anti-BrdU antibody, samples were treated

with fluorescent secondary antibody for 30 minutes. Following three PBS washes, samples were explored to 0.25% Sudan Black B to minimize autofluorescence. Subsequently, PBS washes were performed before covering with fluorescence mounting reagent.

Streptozotocin treatment to induce mouse diabetes

To induce mouse diabetes, mice were intraperitoneally injected with 40 mg/kg streptozotocin (STZ, Sigma-Aldrich) per day for five days, following a protocol established previously[1]. STZ solution was freshly prepared from STZ stock solution with a concentration of 6 mg/mL in 50 mM of sodium citrate buffer (pH 4.5). Mice then received a standard diet with 10% sucrose water. Five days after the treatment with STZ injection and 10% sucrose water, the mice were supplied with regular water.

Lentiviral particle preparation and infection

The small hairpin RNAs [shHepsin #1 (TRCN0000054789) and shHepsin #2 (TRCN0000054790)] for HEPSIN depletion were obtained from the National RNAi Core Facility of Academia Sinica, Taiwan. An shRNA against luciferase (shLuc) was used as a control. Lentivirus was produced from the HEK293T transfectants with co-transfection of pCMVdR8.91, pMD.G, and pLKO.1-puro shRNA plasmids (with a ratio of 9: 1: 10) using Lipofectamine 3000 (DNA: liposome = 5 μg: 15 μL), according to the recommended protocol (Invitrogen, CA, USA). The conditioned media of the

transfected cells containing lentiviral particles were collected at 48 hours. For infection, NIT-1 cells were seeded with a density of 1×10^6 cells per 60-mm culture dish, and 50% (v/v) of the lentivirus-containing medium was added in a regular culture medium. After incubation for 48 hours, the cells were subjected to Western Blot assay.

Human pancreatic tissues

The Department of Pathology, National Taiwan University Hospital (NTUH) provided archived human pancreas tissues with the approval of the Research Ethics Committee of NTUH (case number: 202306101RINB). Written informed consent was obtained from all patients, and the protocol followed the Declaration of Helsinki. These archived human pancreatic tissues were obtained from patients previously admitted to NTUH, diagnosed with benign pancreatic neoplasms, and undergoing pancreatectomy; thirty-nine had diabetes, while twenty-seven did not.

Supplementary Table

Supplementary Table S1

Table S1. Primers used to Southern Blot and Genotyping

Southern Blot probe (5'-3')	TCAACCTTGATTTTAGCCAAGAGTGACTTTGAACTCCTGATCTTCCTGCC

	length (bp)	Forward primer (5'-3')	Reverse primer (5'-3')
Spint1-lacZ	461	CAGGTGAAGGAAGCCTCAAG	AGAGGGACCTGGCTCCTATG
Spint1	656 (for wild-type *Spint1*) 690 (for *loxP* floxed *Spint1*)	GTCCAGCCCATCTTTAGCAG	ACCGTAAACGAGACGAGTGG
Cre	280	ATGCTTCTGTCCGTTTGCCG	TGAGTGAACGAACCTGGTCG

Supplementary Table S2

Table S2. Primers used to qPCR

mouse	Forward primer (5'-3')	Reverse primer (5'-3')
Spint1	CCGAAGGAGGGCTTCATCAAC	GTTCAGTACCAGGGGCTTCTGC
Mafa	TTCAGCAAGGAGGAGGTCAT	CCGCCAACTTCTCGTATTTC
Hepsin	TACCTTCCCTTTCGAGACCCT	CCATAGAACTGTGTGTTACCCCA
St14	CGCGGGACTCAAGTACAACTCC	GCCTCGCTTCTCCACTTTCTTG
Tmprss15	GCTGTGTGCGTTTTCTTAATGG	GCACTCCCTAGTCCCAGAAGAT
Tmprss7	TGTTGGAATGTTCCGCATCAC	GGTTTACCACTTGCTGTACTGT
Tmprss4	CAACCCCTCAACAACCGTGAT	CTCAGCAGCACTGCAATGAT
Tmprss2	ATGCTCCGAGGATTACAACGC	CGAGGGCTAAACACAGCGATT
Ins1	GGGGAGCGTGGCTTCTTCTA	ACCTCCAACGCCAAGGTCTG
Ins2	GGGGAGCGTGGCTTCTTCTAC	CCACCTCCAGTGCCAAGGTC
Gapdh	AGGTCGGTGTGAACGGATTTG	GGGGTCGTTGATGGCAACA

human	Forward primer (5'-3')	Reverse primer (5'-3')
SPINT1	GACTTGAAGGTACAACCCCAG	TGGGTGGTCTGAGCTAGTCAC
MAFA	AGCGAGAAGTGCCAACTCC	TTGTACAGGTCCCGCTCTTT
HEPSIN	CCCCTGCCCCTCACAGAATA	AGTCAGCGCCATTGCAGAC
INS	ACGAGGCTTCTTCTACACACCC	TCCACAATGCCACGCTTCTGCA
GAPDH	AAAGGATCCACTGGCGTCTTCACCACC	GAATTCGTCATGGATGACCTTGGCCAG

Supplementary Table S3

Recombinant protein and antibody used

	company	**Catalog No.**	**Purpose**	**Conditions**
Rt-mSPINT1 protein	R&D	1141-PI-010	Cell treatment	0, 0.4, 0.8, and 1.6 μg/mL
His-tag monoclonal antibody	ProteinTech	66005-1-Ig	Western blot	1:100 in 5% Milk

Reference

1. Wu KK, Huan Y. Streptozotocin-Induced Diabetic Models in Mice and Rats. *Current Protocols in Pharmacology*, (2008).